

Helical piles – An effective foundation system for solar plants

Mohammed Sakr

Worley Parsons Canada, Edmonton, Alberta, Canada

ABSTRACT

Solar energy is a renewable energy that combats climate change, and assures a sustainable energy source. When the Ontario Government introduced the Clean Energy Act in the spring of 2009, an abundance of alternate energy projects were developed for the province. This paper presents the results of two helical pile load testing programs carried out in Canada and the USA. The helical pile load testing programs included axial compression, tension (uplift), and lateral load tests performed in silty clay (cohesive soils) and compact sand (cohesionless soils). A total of nine pile load tests were performed including, one axial compression test, three axial tension tests, and five lateral load tests. The results of pile load test programs and field monitoring of helical piles are summarized in this paper. Soil stratifications and ground water conditions are also documented. The results of the load tests are compared to the theoretical models for estimating their capacities. Torque-pile capacity correlations are also discussed based on the load test results.

1 INTRODUCTION

Driven by climate change mitigation policy and the growing demand for sustainable energy, energy production from renewable sources has become a focal interest of industry and governments. Ontario is leading the country in this area, which led to an electricity surplus in 2010. The growing trend of creating renewable energy infrastructure, such as solar farms and wind turbines, had generated a unique opportunity for geotechnical engineers in terms of providing foundation options that are cost-effective, quick to install, and environmentally friendly.

This paper highlights some of these challenges and addresses the opportunities for helical piles as an alternative foundation option that can minimize the performance disadvantages of traditional foundations. Helical pile load tests performed in cohesive soils and cohesionless soils are presented in this paper. A total of nine static axial tests, including one axial compression test, three axial tension (uplift) tests, and five lateral load tests, were carried out at two sites. The results of a helical pile load test program carried out in silty clay (cohesive soils) for the Arnprior Solar Farm Foundations, Arnprior, Ontario are referred to as Site 1. The results of a helical pile load test program carried out at a solar plant located in Upton, NY in compact sand (cohesionless soils) are referred to as Site 2.

2 SITE DESCRIPTION

2.1 Site 1

The project is located at the intersection of Highway 17 and Galetta Side Road in the town of Arnprior, Ontario. The Arnprior solar farm comprises installation of about 330,000 solar PV modules on an aluminum/steel racking system supported on helical piles. The total capacity of the solar farm is about 21 MW. The site comprises approximately 100 acres and was relatively flat.

The generalized stratigraphy at Site 1 consisted of a thin layer of topsoil, about 150 mm thick underlain by a firm to very stiff silty clay extending to the end of the test holes at a depth of about 5 m. The undrained shear strength of the silty clay layer varied between 43 kPa and 150 kPa. The natural moisture content of the silty clay material varied between 22 and 58 percent. Its unit weight varied between 16.7 and 18.8 kN/m³. Its liquid and plastic limits varied between 35 and 54 percent and 18 to 24 percent, respectively, resulting in a plasticity index range between 17 and 30 percent. Grain size analyses indicate a gradation of 52 to 63 percent clay, 35 to 42 percent silt, and 2 to 5 percent sand. The groundwater level was relatively shallow and varied between 0.6 m and 1.4 m below existing ground surface.

2.2 Site 2

Site 2 is located in Brookhaven, Upton, NY. The results of geotechnical investigation at site 2 indicate that the subsurface conditions were fairly consistent across the solar plant site. A thin topsoil layer was encountered, underlain by alluvial soil layers with intermittent loose zones. Two alluvial soil layers were identified, including an upper deposit, consisting of silt and sand mixture with varying amounts of gravel and clay, and a lower deposit, consisting of compact sand with varying amounts of gravel and silt. Groundwater was encountered at about 1.5 m below existing ground surface. SPT blow count varied between 9 and 24 blows per 300 mm of penetration, indicating a loose to compact sand state.

3 DESIGN CONSIDERATIONS

Solar racks are lightly loaded structures and typically mounted above ground surface at heights varying between 1.2 m to 3.0 m depending on the size of rack, inclination angle, and topography of the solar plant site. Therefore, additional moments due to the free lengths above grade have to be accounted for in foundation design. Moreover, for solar farms constructed in cold climate regions, foundations must be designed considering seasonal frost effects and additional tension loads due to frost heave potential. Frost penetration depths are a function of several parameters, such as average freeze index, soil type, service life of the project, and site surface conditions (i.e. insulation, snow cover, and traffic volume). For example, at site 1, with silty clay soils, the estimated average depth of frost penetration is about 2.1 m if the site is covered with snow and is 2.4 m if snow is removed from the vicinity of the foundations. At test site 2, the estimated frost penetration depth is about 0.9 m. Other factors that contribute to the selection of the foundation option for solar plants may include construction rate, precision in terms of horizontal and vertical alignment, and environmental impact.

Typical foundation options for solar plants may include concrete ballast, driven pile, drilled shaft, and helical piles. Helical pile foundations were selected for both sites due to their cost-effectiveness and speed of installation. Helical piles provide a cost-effective solution for solar farms in cold climates due to their high uplift capacities and shorter lengths compared to driven piles. They are also quick to install, with an average construction rate of more than 100 piles per crew per day (10 working hours).

4 HELICAL PILE CONFIGURATIONS

Piles tested at Site 1 were either single- or double-helix piles (pile types SP1 and SP2) with a shaft diameter of 89 mm, a wall thickness of 6.5 mm, a length of 4.5 m, a helix diameter of 304 mm, and a helix thickness of 9.5 mm. Figure 1 shows details of test pile configurations while Table 1 summarizes the pile configurations.

At site 2, three different pile configurations were considered, including pile types SP3, SP4, and SP5. Piles SP3 and SP4 were single-helix piles with shaft diameters of 114 mm and 168 mm respectively. Pile types SP4 and SP5 had the same shaft diameter of 168 mm. However, pile type SP4 had a single helix while pile type SP5 had double helices. The screw piles tested in this program were manufactured and installed by ALMITA Piling Inc. of Ponoka, Alberta.

Table 1. Helical pile geometry

Pile Type	L m	Shaft		Helices		
		d mm	t_s mm	D mm	t_h mm	No of helices
SP1	4.5	89	6.5	304	9.5	1
SP2	4.5	89	6.5	304	9.5	2
SP3	4.6	114	6.5	304	12.7	1
SP4	4.6	168	7.1	406	12.7	1
SP5	4.6	168	7.1	304	12.7	2

L denotes overall pile length;
d and t_s denote shaft diameter and wall thickness in mm;
D and t_h denote helix diameter and thickness in mm.

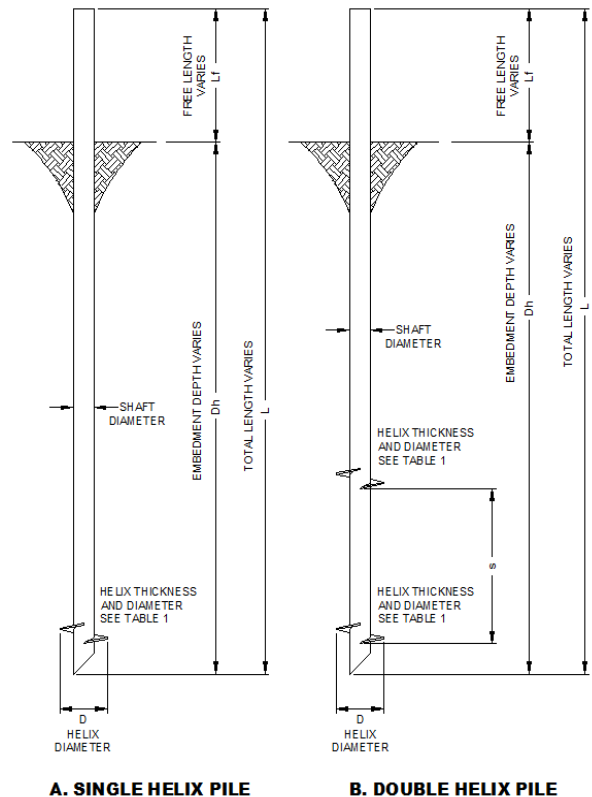


Figure 1. Typical helical pile configuration

5 INSTALLATION MONITORING

The pile installation equipment comprised of a drive unit mounted on an excavator or bobcat. The drive unit contained a hydraulic motor providing the torque for rotation of the screw pile into the ground to a maximum torque of 16.3 kN.m (12,000 ft-lbs) for Site 1 and 135.6 kN.m (100,000 ft-lbs) for Site 2. Summary of pile installation records, including the average torque recorded at the last 0.5 m of installed pile depth and the depth of embedment, are provided in Table 2.

At Site 1, a gradual increase in torque values was observed up to the end of installation, at a depth of about 3.05 m. The measured average torque values at the last 0.5 m of pile installation for different piles were consistent and varied between 5.2 kN-m (3,815 ft-lbs) and 5.5 kN-m (4,000 ft-lbs). This observation indicates that the soil conditions within the installed depth of helical piles were relatively consistent at the pile load test locations.

At Site 2, all piles were embedded to depths varying between 2.1 m and 2.6 m below existing ground surface. It can be seen from Table 2 that the torque values at the end of installation of pile type SP3 with a shaft diameter of 114 mm was about 29.8 kN.m (22,000 ft-lbs). The measured torque values for pile type SP4 with a shaft diameter of 168 mm were 29.8 kN.m (22,000 ft-lbs) and 26.8 kN.m (19,800 ft-lbs). Comparing installation records for pile type SP4 with a single helix and pile type SP5 with double helices indicates that piles T3 and L5 with double helices exhibited slightly lower torque values than piles T2 and L4 with a single helix (26.8 kN.m (19,800 ft-lbs) vs. 29.8 kN.m (22,000 ft-lbs)). The lower torque values of pile type SP5 with double helices are due to their smaller helix diameter.

Comparing piles installed in cohesive soils at site 1 and cohesionless soils at site 2 indicates that the torque requirement for installing piles in cohesionless soils was considerably higher than the torque requirement for installation in cohesive soils.

Table 2. Summary of pile installation

Site ID	Test ID	Pile Type	Installation Torque at end of installation kN.m	Embedment Depth m
Site 1	C1	SP1	5.3	3.05
	T1	SP1	5.5	3.05
	L1	SP1	5.2	3.05
	L2	SP2	5.3	3.05
Site 2	L3	SP3	29.8	2.6
	T2	SP4	29.8	2.1
	L4	SP4	32.8	2.1
	T3	SP5	26.8	2.3
	L5	SP5	26.8	2.1

6 LOAD TEST SETUP

The axial compression and tensile load tests were carried out in accordance with ASTM standards D 1143-07 and D 3689-07. Since the main objective of the load tests was to determine the ultimate bearing capacity of the pile, a Procedure A (Quick Test) was adopted for the tests, wherein numerous small load increments were applied and maintained constant over short time intervals. The lateral pile load tests were carried out using Procedure A in accordance with ASTM standards D 3966-07. The typical test setups for axial compression and lateral tests are shown in Figures 2 and 3. For axial compression and tension tests, pile head axial movements were monitored at four points during the test, using two independently supported Linear Displacement Transducers (LDT), with 0.05 mm accuracy and 150 mm travel, and two mechanical dial gauges (0.05 mm accuracy- 150 mm travel). Another two LDTs were installed to monitor lateral movement in both longitudinal and transverse directions near the pile head. All LDT readings were also recorded automatically at time increments of 30 seconds throughout the test duration.



Figure 2. Typical axial compression test setup



Figure 3. Typical lateral load test setup

For lateral load tests at site 1, loads were applied at about 200 mm above ground surface, and horizontal movements were monitored at three points along the pile free length (at distances of 200 mm above ground surface) to measure lateral deflections at point of load application and at a distance of about 1500 mm above ground. For lateral load tests at site 2, loads were applied at about 1750 mm above ground surface and horizontal movements were monitored at distances of about 200 mm and 1750 mm above ground surface.

7 TEST RESULTS

7.1 Site 1

7.1.1 Axial Compression Test Results

The load displacement curve for the compressive load test for pile C1 is presented in Figure 4. It can be seen from Figure 4 that the load displacement curve can be characterized into three parts. The first part is linear up to a displacement of about 0.5 mm. The second part is a non-linear behaviour up to a displacement of about 24 mm that corresponds to the failure of the soil in helix zone (end bearing resistance). The third part is a near horizontal component that corresponds to plunging failure. The load at the pile head at the end of the initial linear component was about 40 kN, and the load at the beginning of the second linear component was about 115 kN.

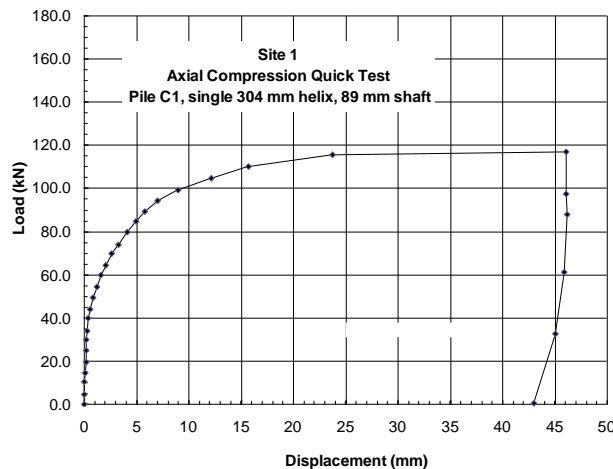


Figure 4. Load displacement curve for axial compression load test - Site 1

Sakr (2008) defined the ultimate capacity of a helical pile as the load that corresponds to the displacement at the pile head equal to 5% of the helix diameter. The 5% failure criterion provides a reasonable estimate of the ultimate capacity of helical piles at a reasonable displacement level. The ultimate load capacity for pile C1, determined using the 5% criterion, was 109 kN.

7.1.2 Axial Tensile Test Results

The results of the uplift load test for pile T1 at site 1 is presented in the form of a load displacement curve in Figure 5. The curve is used to determine the ultimate tension (uplift) load capacity. It can be seen from Figure 5, as with to compression tests, the load displacement curve can be characterized into three parts: a first linear part up to a displacement of about 0.5 mm, followed by a non-linear component up to a displacement of about 14 mm, and a secondary linear component with a near horizontal slope. The load at the pile head at the end of the initial linear component was about 35 kN, and the load at the beginning of the second linear component was about 75 kN. The ultimate tensile (uplift) capacity of helical pile T1, estimated using the 5% failure criterion, was about 70 kN.

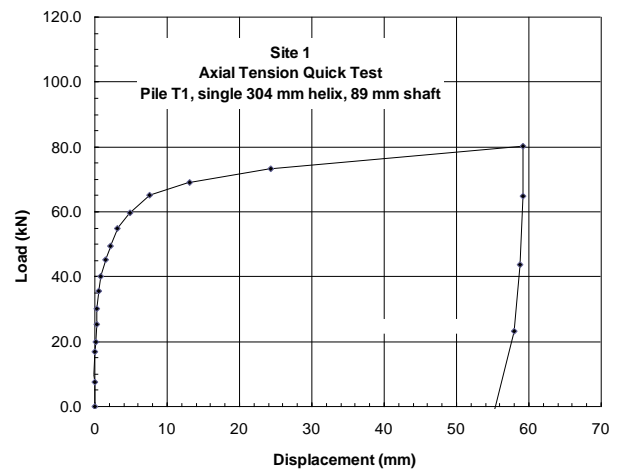


Figure 5. Load displacement curve for axial tension test - Site 1

7.1.3 Lateral Load Test Results

The results of lateral load tests for test piles L1 and L2 are presented in the form of load deflection curves in Figure 6. Pile L1 had a single helix; while pile L2 had double helices. Other configurations of both piles were the same. It can be seen from Figure 6 that the lateral responses of both piles were non-linear. Gaps were formed behind the piles during testing, indicating a plastic deformation of the soil in front of the pile within the upper soil layers. It can be seen from Figure 6 that both piles showed similar resistances and that the lateral resistance of pile L2 was about 4 to 6% higher than that of pile L1. This observation indicates that the number of helices had a minor effect on the lateral resistance of piles tested at site 1.

Pile L1 was loaded to a maximum load of about 21 kN, which corresponded to a maximum deflection of about 42 mm, while pile L2 was loaded to maximum load of 22 kN, which corresponded to a maximum deflection of 41 mm. When piles L1 and L2 rebounded to zero load, the net or permanent displacement was about 5 mm for both piles. The lateral loads at deflection levels of 6, 12,

and 25 mm, for pile L1 were 5.5, 8.8, and 14.7 kN, respectively. The lateral loads at deflection levels of 6, 12, and 25 mm, for pile L2 were 6.0, 9.8, and 16.2 kN, respectively.

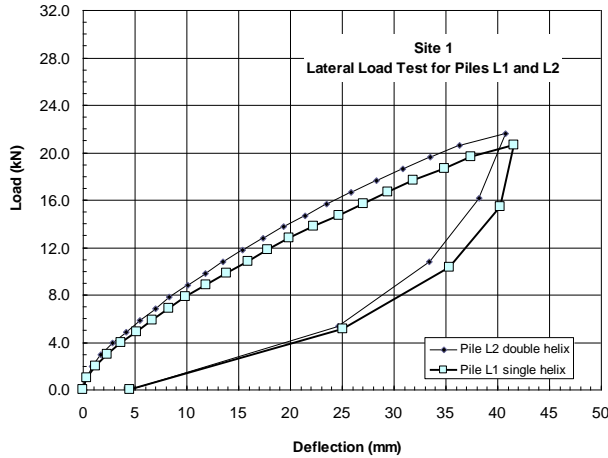


Figure 6. Load deflection curves for lateral load tests - Site 1

7.2 Site 2

7.2.1 Axial Tensile Test Results

The results of uplift load tests for piles T2 and T3 are presented in the form of load displacement curves in Figure 7. It can be seen from Figure 7 that the load displacement curves can be characterized into three parts: a first linear part up to a displacement of 2 mm, followed by non-linear component up to a displacement of about 20 mm and 35 mm, and secondary linear component with a near-horizontal slope. The maximum uplift loads for pile T2 with single helix and pile T3 with double helices were about 104 kN and 90 kN, respectively, and plunging failure was observed for both piles. The maximum displacements at the end of loading were about 85 mm and 77 mm.

The load displacement curves for pile T2 with a shaft diameter of 168 mm and a single helix 406 mm in diameter (pile type SP4) and pile T3 with the same shaft diameter of 168 mm and double helices 304 mm in diameter (pile type SP5) (Figure 7) were similar up to a load of about 45 kN and a corresponding displacement of about 2 mm. However, at higher displacement levels, pile T2 with a single helix offered higher resistance than pile T3 with double helices. This observation suggests that it is not necessarily that the double-helix pile performs better than the single-helix pile. The higher resistance of pile T2 is likely due to the larger size of its helix and increased embedment depth. However, for pile T3, although it had two helices, the size of the helices was smaller (i.e. 304 mm), and the upper helix did not fully mobilize its end bearing resistance due to its shallow embedment depth.

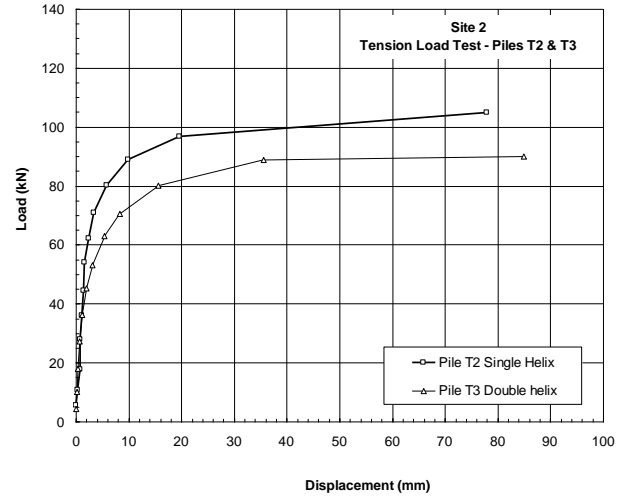


Figure 7. Load displacement curve for axial tension tests - Site 2

7.2.2 Lateral Load Test Results

The results of lateral load tests for test piles L3 and L4 are presented in the form of load deflection curves in Figure 8. It should be noted that lateral deflections were measured at the point of load application at about 1.75 m above ground to represent the deflection at the connection between piles and the rack of the solar panel. It can be seen from Figure 8 that the lateral responses of both piles were non-linear. The lateral resistance of pile L4 with a shaft diameter of 168 mm was considerably higher than that of pile L3 with shaft diameter of 114 mm.

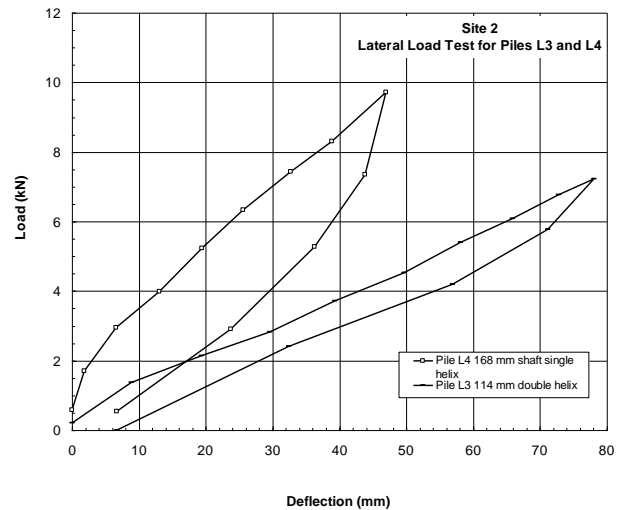


Figure 8. Lateral load deflection curves for piles L3 and L4 - Site 2

The load deflection curves for piles L4 and L5 with the same shaft diameter of 168 mm and with single and double helices (i.e. types SP4 and SP5) are plotted in Figure 9. It can be seen from Figure 9 that the lateral response of pile L4 with a single helix was stiffer than that of pile L5 with double helices, being manifested in lower deflections at the same lateral load levels. For example, the lateral deflection at a load level of about 9 kN was about 47 mm for pile L4 and 58 mm for pile L5. A possible reason for the softer response of pile L5 with a double helix is the higher soil disturbance level compared to pile L4 with a single helix. The maximum difference between the lateral resistances of piles L4 and L5 was about 20%.

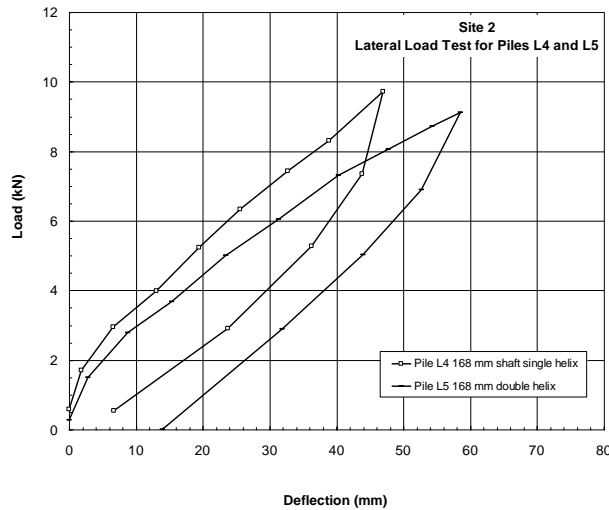


Figure 9. Lateral load deflection curves for piles L4 and L5 - Site 2

8 COMPARISON BETWEEN MEASURED AND ESTIMATED AXIAL CAPACITIES

The capacity of helical piles can be determined based on the bearing capacity theory using the individual helix method. In the individual helix method, the ultimate axial capacity of the pile is the sum of the individual bearing capacities of all helices. The major factors that affect the vertical capacity are the pile geometry (diameter, depth and spacing of helices), the soil and groundwater profile, and the installation procedures.

8.1 Site 1 (Cohesive Soils)

8.1.1 Axial Compressive Capacity

The axial compressive capacities of helical piles with a single helix, installed in cohesive soils, may be estimated as follows:

$$Q_c = A_H C_u N_c + \pi d H_{eff} \alpha C_u \quad [1]$$

where:

Q_c = ultimate screw pile compressive capacity, (kN)

A_H = net area of helix, (m^2)

C_u = undrained shear strength of soil layer, (kPa)

N_c = dimensionless bearing capacity factor

d = diameter of the shaft, (m)

H_{eff} = effective length of pile, $H_{eff} = H - D$, (m)

α = Adhesion factor

The estimated axial compressive capacity of pile C1 is presented in Table 3. The axial capacity was assessed using the soil profile presented in Section 2.1 with the following parameters:

- For soil layer up to a depth of 2 m: undrained shear strengths of 60kPa; total unit weight of 18 kN/m³ above groundwater level and effective unit weight of 8.2 kN/m³ below groundwater level; and
- For soil layer below a depth of 2 m: undrained shear strengths of 70kPa; and effective unit weight of 8.2 kN/m³.

The estimated capacity of pile C1 was about 25% lower than the measured values.

Table 3. Comparison between measured and estimated capacities

Pile ID	Ultimate Pile Capacity Measured Q_{ult} , kN	Ultimate Pile Capacity Estimated Q_{ult} , kN	Prediction Ratio	Torque Factor, K_t m ⁻¹
C1	109	81.6	0.75	20.6
T1	70	70	1.0	12.7
T2	93	99	0.94	3.1
T3	80	87	0.92	3.7

8.1.2 Axial Tensile Capacity

For predicting the total uplift capacity for pile T1 for cohesive soils encountered at site 1, the following expression may be used:

$$Q_t = A_H (C_u N_u + \gamma' H) + \pi d H_{eff} \alpha C_u \quad [2]$$

where:

Q_t = ultimate screw pile uplift capacity, (kN)

A_H = net Area of helix, (m^2), area of the helix – area of pile shaft

γ' = effective unit weight of soil, (kN/m³)

N_u = dimensionless uplift bearing capacity factor for cohesive soils

H = embedment depth, (m)

The estimated axial uplift capacity for pile T1 compared well with the measured capacity (see Table 3).

8.2 Site 2 (Cohesionless Soils)

8.2.1 Axial Tensile Capacity

The uplift capacities for helical piles installed in cohesionless soils at site 2 may be estimated using Eqn 3, below.

$$R = \sum Q_h + Q_f \quad [3]$$

The individual helix uplift capacity, Q_h , can be estimated using Eqn 4 (Das, 1990) listed below.

$$Q_h = A_h \gamma D_h F_q \quad [4]$$

where

D_h = depth to helical bearing plate

F_q = Breakout Factor.

The breakout factor, F_q , is defined as the ratio between the uplift bearing pressure and the effective vertical stress at the upper helix level. The following expression can be used to estimate the breakout factor (Das and Seeley, 1975):

$$F_q = 1 + 2 \left[1 + m \left(\frac{D_h}{D} \right) \right] \left(\frac{D_h}{D} \right) K_U \tan \phi \quad ; \text{ where}$$

$$\left(\frac{D_h}{D} \right) \leq \left(\frac{D_h}{D} \right)_{cr} \quad [5]$$

where

m = coefficient dependent on soil friction angle

D_h = embedment depth to the upper helix;

D = diameter of the upper helix

K_U = nominal uplift coefficient

ϕ = average frictional resistance angle for the soils above the upper helix

$\left(\frac{D_h}{D} \right)_{cr}$ = critical embedment ratio

The breakout factor, F_q , depends on several parameters such as the embedment depth ratio (D_h/D), the weight of the soil above the upper helix, shape of the helix, and the angles of internal friction for the soils above the upper helix. It can be seen from Eqn 5 that the F_q increases with embedment ratio until the critical embedment ratio, after which the F_q is independent of embedment depth. The estimated critical embedment ratio, $\left(\frac{D_h}{D} \right)_{cr}$, for the compact sand layer above the upper helix considered in the present study was about 7.

The estimated axial uplift capacities of piles T2 and T3 are also presented in Table 3. The estimated capacities were also compared to the measured capacities using the

5% criterion. It should be noted that the ratio between the estimated and measured capacities varied between 0.92 and 1.19, which indicates that the individual helix method can be used to assess pile capacities with a reasonable accuracy.

9 TORQUE CAPACITY RELATIONSHIP

A simple empirical relation between torque and ultimate pile capacity has been established. It has been statistically analyzed based on a large database, and the method has been used successfully in the construction of thousands of anchors over the past twenty years as indicated by Hoyt et al. (1995). The empirical relationship can be expressed as (Hoyt and Clemence, 1989; CFEM, 2006):

$$Q_t = K_t T \quad [6]$$

where

Q_t = ultimate capacity of screw pile;

K_t = empirical factor; and

T = average installation torque

It should be noted that torque-load correlations reported in the literature are established for small-diameter anchors resisting uplift loads. Torque exerted during pile installation is dependent on several factors, such as the operator experience, vertical forces exerted on the pile during installation, shape of the pile shaft (i.e. circular or square), helix shape, pitch size, number of helices, method of torque measurements, and frequency of calibrating the equipment. In addition to that, for the case of helical piles installed to resist compression loads, torque reported during installation cannot predict the strength of the soil layer immediately below the lower helix that will considerably impact the compressive strength of helical piles. Therefore, it is suggested to not rely on torque factor as a design tool. However, torque factor can be used to qualitatively assess the relative strength of the soils during the construction phase.

The measured empirical factor, K_t , for compression and tension tests at site 1, was 20.6 and 12.7 m^{-1} for piles C1 and T1. Empirical K_t factor in compression was considerably higher than that factor in tension. The measured K_t value of 12.7 m^{-1} is considerably lower than the recommended value of 23 m^{-1} in the CFEM (2007). The K_t values for tension tests for piles T2 and T3 at site 2 were 3.1 and 3.7 m^{-1} , respectively which are considerably lower than empirical factors for site 1. Possible reasons for such large differences are soil conditions (i.e. clay material versus sand material), pile sizes, helices sizes and number of helices. As with site 1, the measured K_t values for site 2 were considerably lower than the recommended value in the CFEM of 10 m^{-1} .

10 CONCLUSIONS

Helical piles provided an effective foundation option for both sites considered in the study in terms of the speed of installation to meet tight schedules, positioning accuracy and their high tensile capacities. The test results can be summarized as follows:

1. Helical piles installed in compact sand (cohesionless soils) required more torque than piles installed in clay soils (cohesive soils).
2. The load-displacement curves for piles subjected to compression and uplift loads indicate that a typical trend consisted of an initial linear segment followed by a non-linear segment, followed by an asymptote (plateau).
3. The axial compressive and tensile (uplift) capacities of helical piles installed at sites 1 and 2 may be estimated using the individual helix method.
4. Helical piles can resist lateral loads and moments in cohesive and cohesionless soils. However, for design of solar panel foundations, considerations should be given to design lateral loads, moments, and performance requirements in terms of maximum allowable horizontal deflections.
5. Helical piles with either single or double helices provided similar lateral resistance depending on the shaft size and embedment depth. However it should be noted that these conclusions is based on limited number of tests at certain sites. Therefore additional research is required to further investigate the effect of multi-helices on their lateral behaviour.

ACKNOWLEDGEMENTS

The author would like to thank Mr. Larry Kaumeyer, president of Almita Piling Inc for permission to use the test data presented in the paper. Thanks are also extended to Mr. Scott Blackie of Almita for his valuable support during the field work.

REFERENCES

ASTM D 1143-81 07. 2007. Standard Test Method for Piles Deep Foundations Under Static Axial Compressive Load. Annual Book of ASTM Standards.

ASTM D 3689-07. 2007. Standard Test Method for Deep Foundations Under Static Tensile Load. Annual Book of ASTM Standards.

ASTM D 3966-07. 2007. Standard Test Method for Deep Foundations under Lateral Load. Annual Book of ASTM Standards.

CFEM. 2006. Canadian Foundation Engineering Manual. 4th Edition. Canadian Geotechnical Society, Technical Committee on Foundations, BiTech Publishers Ltd., Richmond, B.C.

Das, B. M. 1990. Earth Anchors. Elsevier, Amsterdam.

Das, B.M. and Seeley G. R. 1975. Breakout resistance of horizontal anchors. Journal of Geotechnical Engineering Division, ASCE, 101(9): 999–1003.

Hoyt, R.M., and Clemence, S.P. 1989. Uplift capacity of helical anchors in soil. In Proceedings of the 12th International Conference on Soil Mechanics and Foundation Engineering, Rio de Janeiro, Brazil, Vol. 2, pp. 1019-1022.

Hoyt, R., Seider, G., Reese, L. C., and Wang, S. T. 1995. Buckling of helical anchors used for underpinning: Foundation upgrading and repair for infrastructure improvement. Edited by William F. K. and Thaney, J. M. Geotechnical Special Publication No. 50, ASCE, pp. 89-108.

Sakr, M. 2008. Performance of Helical Piles in Oil Sand. 61st Canadian geotechnical Conference and 9th Joint CNL Groundwater Conference, Edmonton, Alberta, September 21 – 24, 2008, pp. 55-62.